# A defect of amphiregulin release predicted longer survival independently of YAP expression in patients with pleural mesothelioma in the IFCT -0701 MAPS phase 3 trial

Elodie Maille, Jérôme Levallet, Fatéméh Dubois, Martine Antoine, Claire Danel, Christian Creveuil, Julien Mazieres, Jacques Margery, Laurent Greillier, Valérie Gounant, et al.

Received: 4 September 2021 | Revised: 12 February 2022 | Accepted: 22 February 2022

DOI: 10.1002/ijc.33997

MOLECULAR CANCER BIOLOGY

IJC INTERNATIONAL JOURNAL of CANCER

# A defect of amphiregulin release predicted longer survival independently of YAP expression in patients with pleural mesothelioma in the IFCT-0701 MAPS phase 3 trial

Elodie Maille[1] | Jérôme Levallet[1] | Fatéméh Dubois[1,2] | Martine Antoine[3] | Claire Danel[4] | Christian Creveuil[1,5] | Julien Mazieres[6] | Jacques Margery[7] | Laurent Greillier[8] | Valérie Gounant[9,10] | Denis Moro-Sibilot[11] | Olivier Molinier[12] | Hervé Léna[13] | Isabelle Monnet[14] | Emmanuel Bergot[1,15] | Alexandra Langlais[16] | Franck Morin[16] | Arnaud Sherpereel[17] | Gérard Zalcman[10,18] | Guénaëlle Levallet[1,2]

[1]Normandie Univ, UNICAEN, CNRS, ISTCT-UMR6030, Caen, GIP CYCERON, France

[2]Department of Pathology, CHU de Caen, Caen, France

[3]Department of Pathology, Hôpital Tenon, AP-HP, Paris, France

[4]Department of Pathology, Hôpital Bichat-Claude Bernard, AP-HP, Université Paris-Diderot, Paris, France

[5]Biomedical Research Unit, CHU de Caen, Caen, France

[6]Department of Pulmonology, Hôpital Larrey, CHU de Toulouse, Toulouse, France

[7]Department of Medical Oncology, Institut Gustave Roussy, Villejuif, France

[8]Department of Multidisciplinary Oncology and Therapeutic Innovations, Assistance Publique Hôpitaux de Marseille, Université Aix-Marseille UM015, Marseille, France

[9]Department of Pulmonology, Hôpital Tenon, AP-HP, Paris, France

[10]Department of Thoracic Oncology & CIC 1425, University Hospital Bichat-Claude Bernard, AP-HP, Université de Paris, Paris, France

[11]Pôle Thorax et Vaisseaux, University Hospital of Grenoble-Alpes, La Tronche, France

[12]Department of Pulmonology, Centre Hospitalier Le Mans, Le Mans, France

[13]Department of Pulmonology, University Hospital Pontchaillou, Rennes, France

[14]Department of Pulmonology, Centre Hospitalier Intercommunal de Créteil, Créteil, France

[15]Department of Pulmonology and Thoracic Oncology, University Hospital of Caen, Caen, France

[16]Intergroupe Francophone de Cancérologie Thoracique (IFCT), Paris, France

[17]Department of Pulmonary and Thoracic Oncology, Centre Hospitalier Universitaire Lille, University of Lille, U1019 INSERM, Center of Infection and Immunity of Lille, Lille, France

[18]U830 INSERM, "Cancer, Hétérogénéité, Instabilité et Plasticité" Centre de Recherche, Institut Curie, Paris, France

**Abbreviations:** ANOVA, one-way analysis of variance; AREG, amphiregulin; BrdU, bromodeoxyuridine; EMT, epithelial-mesenchymal transition; MAPS, Mesothelioma Avastin Cisplatin Pemetrexed Study; MPM, malignant pleural mesothelioma; OS, overall survival; PFS, progression-free survival; PMA, phorbol 12-myristate 13-acetate; SDC1, syndecan-1; TACE, tumor necrosis factor-alpha-converting enzyme.

Elodie Maille, Jérôme Levallet, Gérard Zalcman and Guénaëlle Levallet contributed equally to our study.

**Correspondence**
Guénaëlle Levallet, ISTCT-UMR6030, Avenue H. Becquerel, 14074 Caen, France.
Email: guenaelle.levallet@unicaen.fr

**Funding information**
The Bio-MAPS study was sponsored by the *Intergroupe Francophone de Cancérologie Thoracique* (IFCT), and funded by an unrestricted research grant from ROCHE-France, research grants from ROCHE-France (2013) and from the Fond de Recherche en Santé Respiratoire (FRSR, 2012) to Guénaëlle Levallet, a research grant "APRI" from Caen University Hospital for S. Brosseau (2014), and a research grant from the Normandie League against cancer for G. Zalcman (2012).

## Abstract

The Hippo pathway effector YAP is dysregulated in malignant pleural mesothelioma (MPM). YAP's target genes include the secreted growth factor *amphiregulin* (AREG), which is overexpressed in a wide range of epithelial cancers and plays an elusive role in MPM. We assayed the expression of YAP and AREG in MPM pathology samples and that of AREG additionally in plasma samples of patients from the randomized phase 3 IFCT-0701 Mesothelioma Avastin Cisplatin Pemetrexed Study (MAPS) using immunohistochemistry and ELISA assays, respectively. MPM patients frequently presented high levels of tumor AREG (64.3%), a high cytosolic AREG expression being predictive of a better prognosis with longer median overall and progression-free survival. Surprisingly, tumor AREG cytosolic expression was not correlated with secreted plasma AREG. By investigating the AREG metabolism and function in MPM cell lines H2452, H2052, MSTO-211H and H28, in comparison with the T47D ER+ breast cancer cell line used as a positive control, we confirm that AREG is important for cell invasion, growth without anchorage, proliferation and apoptosis in mesothelioma cells. Yet, most of these MPM cell lines failed to correctly execute AREG posttranslational processing by metalloprotease ADAM17/tumor necrosis factor-alpha-converting enzyme (TACE) and extracell secretion. The favorable prognostic value of high cytosolic AREG expression in MPM patients could therefore be sustained by default AREG posttranslational processing and release. Thus, the determination of mesothelioma cell AREG content could be further investigated as a prognostic marker for MPM patients and used as a stratification factor in future clinical trials.

**KEYWORDS**
amphiregulin, malignant pleural mesothelioma, YAP

### What's new?

Malignant pleural mesothelioma (MPM) is an aggressive cancer, for which novel markers and therapeutic strategies are needed. Here, in MPM tumor specimens and controls, the authors investigated the prognostic potential of amphiregulin (AREG), a target of the transcriptional coactivator YAP, which drives MPM progression. Relative to controls, MPM patients with high cytosolic AREG expression had better prognosis, with longer survival. Analyses suggest that high cytosolic AREG expression results from sustained default AREG post-translational processing and release. AREG tumor expression may be a valuable tool for the identification of MPM patients with favorable prognosis, enabling adaptations in their therapeutic care.

## 1 | INTRODUCTION

Several alterations in the Hippo pathway have been reported in malignant pleural mesothelioma (MPM), including LATS2 and NF2 mutations.[1-3] MPM is a rare but aggressive cancer that is mainly caused by occupational asbestos exposure affecting the lung envelope.[4] Indeed, MST1/Hippo promoter gene methylation, resulting in nuclear active YAP accumulation, predicted poor survival in MPM patients enrolled in the phase 3 IFCT-GFPC-0701 Mesothelioma Avastin Cisplatin Pemetrexed Study (MAPS).[2] This is probably because YAP, which is a transcriptional coactivator, causes transcription of genes involved in cell motility, growth, survival and epithelial-mesenchymal transition (EMT).[5] Consistently, in MPM cell lines H2052 and H2452, MST1/Hippo depletion increased nuclear YAP accumulation, with an increased expression of its transcriptional targets *ANKDR1* and *Cyr61*.[3]

*Amphiregulin* (AREG), another target gene of YAP or its ortholog TAZ,[6] encodes a transmembrane precursor protein named pro-AREG.[7] Proteolytic processing and functional activation of pro-AREG is achieved by the metalloprotease ADAM (A disintegrin and metalloproteinase) 10 or ADAM17, also known as tumor necrosis factor-alpha-converting enzyme (TACE).[8] This proteolytic cleavage of pro-AREG leads to the release of the soluble and mature part of AREG (sAREG), which is a ligand of the epidermal growth factor receptor (EGFR) that directly stimulates the EGFR downstream intracellular signaling cascades governing cell survival, proliferation and motility. By its mitogenic action, AREG plays a central role in lung organogenesis.[9] However, it may also act as an oncogene in some cellular contexts.[7] AREG is indeed overexpressed in a wide range of epithelial cancers, including those of the lung[10] and breast,[11] as well as head and neck squamous cell carcinomas (HNSCC).[12] It is also reported to be associated with poor overall survival (OS), especially in HNSCC[13] and nonsmall-cell lung carcinoma (NSCLC).[14] This worse prognostic value has also been found for sAREG quantification in serum.[15,16]

AREG's place in the natural history of MPM remains unknown. AREG stimulates the invasion of MPM cells,[17] and MPM cells were reported to express more AREG and EGFR compared to their normal mesothelial cells' counterparts.[18] This suggests that an excessive EGFR activation loop contributes to the aggressiveness of mesothelioma, while no activating EGFR mutation was ever described in MPM. Moreover, AREG was recently shown to enhance vascular endothelial growth factor (VEGF)-A production and endothelial tube formation and to promote angiogenesis or lymphangiogenesis in different cancer cell models,[19,20] because its expression is up-regulated in hypoxic conditions by the transcription cofactor hypoxia-inducible factor-2 (HIF-2). We herein report in a unique way that AREG expression predicted better survival of MPM patients from the IFCT-0701 MAPS phase 3 trial, which established the efficacy of the anti-VEGF monoclonal antibody bevacizumab in MPM patients.[21] AREG post-translational processing and release were actually shown to be faulty in most MPM cells and can therefore not exercise their mitogenic actions.

## 2 | MATERIALS AND METHODS

### 2.1 | Patients from the MAPS trial

From February 13, 2008, to January 5, 2014, 448 patients were randomly assigned to the experimental arm (pemetrexed plus cisplatin and bevacizumab [CisPem+Beva]) or to the reference arm (pemetrexed plus cisplatin [CisPem]). The main clinical results have been previously reported.[21]

### 2.2 | Cell culture, transfection and treatments

Human MPM cell lines MSTO-211H (RRID:CVCL_1430), NCI-H2452 (RRID:CVCL_1553), NCI-H28 (RRID:CVCL_1555), NCI-H2052 (RRID:CVCL_1518) from the American Tissue Culture Collection (ATCC) and T-47D (RRID:CVCL_0553), a generous gift from Pr Le Romancer (Cancer Research Center, Lyon, France), were maintained in RPMI-1640 medium supplemented with 10% fetal bovine serum, 10 mM L-glutamine, streptavidin/penicillin (100 μg/mL) and kanamycin (100 μg/mL). All human cell lines have been authenticated using short tandem repeat profiling within the last 3 years. All experiments were performed with mycoplasma-free cells.

Cells were transfected with siRNA or plasmid DNA using JetPRIME (Polyplus-transfection), as previously reported[3] (Table S1). Exogenous AREG (20 ng/mL) was added to the cell supernatant 24 hours following the cell transfection or treated with phorbol 12-myristate 13-acetate (PMA, 25 ng/mL) for 30 minutes to 3 hours.

### 2.3 | Real time reverse transcription-polymerase chain reaction

After total RNA extraction, real time reverse transcription-polymerase chain reaction (RT-PCR) was performed on each primer sets (Table S2), as previously described,[22] and normalized to S16. Relative quantification was calculated using the delta-delta-Ct method. Primers used for TACE amplification by RT-PCR and sequencing are listed in Table S3.

### 2.4 | Subcellular fractionation

Cells were trypsinized then Total, Nuclear and Cytosolic enriched fractions were isolated using Abcam's Cell Fractionation Kit (Standard) (ab109719, Abcam) according to manufacturer's instructions. Purity of subcellular fractions were checked by assaying the contamination of a cell compartment by another, detecting in each fraction Histone H3 (a nuclear protein) and GAPDH (a cytoplasmic protein) contents.

### 2.5 | Immunoblotting

Whole-cell protein extracts were prepared as previously described,[22] and proteins detected by immunoblotting with a primary antibody (Table S4) were diluted at 1:1000 in Tween (0.1%)-Tris-buffered saline (TBS) buffer and a horseradish peroxidase (HRP)-conjugated secondary antibody before being revealed using an enhanced chemiluminescence kit (Promega).

### 2.6 | Immunofluorescence and image analysis

Cells were fixed and permeabilized as described previously.[22] Primary antibodies (Table S4) were diluted at 1:100. Secondary antibodies (AlexaFluo, Invitrogen) were added for 1 hour.

Coverslips were mounted with DAPI (Santa Cruz), and images were captured with high-throughput confocal microscopy (FluoView FV1000, Olympus).

## 2.7 | AREG measurements on plasma or cells

Amphiregulin release in the plasma of MPM patients in the IFCT-GFPC-0701 MAPS trial was quantified using the amphiregulin Quantikine ELISA kit (R&D system), according to the manufacturer's instructions.

Amphiregulin that was associated with cells (cellular AREG) or that was released in the culture medium (sAREG) was measured using a DuoSet-ELISA kit (R&D system), according to the manufacturer's instructions.

## 2.8 | Immunohistochemistry

Slides from Tumor paraffin-embedded blocks were pretreated with 0.01 mol/L citrate buffer (pH 6; Dako) for 20 minutes at 100°C, then immunostainings were performed with automated immunohistochemical stainer (Dako). Slides were successively incubated at room temperature in 3% $H_2O_2$ for 5 minutes, then with monoclonal antibody (Table S4) diluted at 1:200 for 60 minutes at room temperature. Finally, antibody fixation was revealed by the EnVision+ Dual Link System (Dako).

The staining intensity was recorded by two expert pathologists (MA and CD) blinded to treatment arm. YAP was scored as 0 (negative), 1 (weak), 2 (moderate) or 3 (strong), at ×40 magnification. An overall IHC composite score was calculated from the sum of the staining intensity (0-3) multiplied by the distribution (0%-100%) from all parts of the slide, giving a H-score between 0 and 300. AREG was scored as negative (no signal despite positive internal control) or positive at ×40 magnification.

## 2.9 | Wound healing

Cells transfected or not with siAREG were grown onto 24-well collagen IV coated plates (BD-BioCoat) were treated with mitomycin C (1 μg/mL) diluted in 1%-FBS medium 12 hours before an artificial "wound" was created at 0 hours. Medium was replaced by 1%-FBS medium containing or not exogenous AREG (20 ng/mL). Photographs were taken (×10) every 30 minutes during 16 hours. Wound closure was expressed as a percentage.

## 2.10 | Invasion

Cells ($15 \times 10^3$ cells) were added into the top invasion chambers of 24-well Transwell plates containing a cell-culture insert (BD-BioCoat Matrigel Invasion Chamber, BD Biosciences). At 48 hours, migrating cells were stained with crystal violet, as previously reported.[3]

## 2.11 | Soft agar assay

A base agar matrix (100 μL, Cell Biolabs) was seeded in a 96-well plate, and 1500 cells/well were layered on agar, followed by 50 μL of 2× complete medium. After 25 days, the colonies were stained and counted for each well.

## 2.12 | Spheroid culture

At 24 hours posttransfection, cells were reseeded with the complete medium in 24-well plates without adhesion (Nunclon Sphera Microplates, Thermo Fisher Scientific). Sphere formation was evaluated on Day 6 at ×10 magnification with a phase-contrast inverted microscope, as previously reported.[3]

## 2.13 | Caspase-3/7 assay

DNA fragmentation and caspase-3/7 activation were assayed using the Cell Death Detection ELISAPLUS kit (Roche, USA) and the Caspase-Glo 3/7 Luminescence Assay (Promega Corp, Madison, WI), respectively, according to the manufacturer's instructions.

## 2.14 | Bromodeoxyuridine incorporation analysis

Cells were transfected, left for 24 hours and then labeled with bromodeoxyuridine (BrdU) (1:500 dilution, cell proliferation assay, Millipore) for a further 24 or 48 hours. BrdU incorporation was measured according to the manufacturer's instructions (Merck Millipore, Germany). The colored reaction was quantified using a microplate reader at 450 nm.

## 2.15 | Statistical analysis

In vitro data are presented as means ± SE of the mean (SEM) ($n \geq 3$). Statistical differences were determined by one-way analysis of variance (ANOVA), followed by Dunnett's multiple comparison test (GraphPad Software, Inc). Statistical significance was set at $P \leq .05$.

The Bio-MAPS study was preplanned, ancillary and purely exploratory. Kaplan-Meier survival curves were calculated, and survival differences were tested using the log-rank test ($P < .05$ was set as the significance level). Additionally, we tested the prognostic effect of AREG and YAP tumor expression and of AREG serum concentration on progression-free survival (PFS) and OS. To this end, we used univariate or multivariate Cox proportional

hazards models, with adjustment for the treatment arm, randomization stratification variables of the MAPS trial (histology, performance status [PS] and smoking status), and clinical risk factors known to be associated with survival (gender, age, hemoglobin, white blood cells and platelets) in the MAPS trial.[21] Interaction tests were used to assess the predictive value of AREG or YAP tumor staining according to the treatment arm of the MAPS trial, which was either CisPem or CisPem+Beva.

Bootstrap resampling was used in 1000 theoretical samples to assess the AREG model's stability. The data were analyzed with IBM SPSS software version 22.0.

## 3 | RESULTS

### 3.1 | Cytosolic tumor expression of AREG predicted longer survival in MPM patients from the IFCT-GFPC-0701 MAPS trial

AREG was assessed in tumor specimens for 306/448 patients (68.3%, Figure S1). For 21 patients, immunohistochemistry was not interpretable (samples damaged or unstuck, Figure S1). The AREG immunostaining was cytoplasmic (Figure 1Ai) and/or nuclear (Figure 1Aii), with rare samples also showing nucleolar staining (not shown). Neither the tumor cell membrane nor extracellular matrix was stained.

The average AREG H-score was 59.87 ± 26.92, and the median score was 70 (30-80). There was no significant difference between the patients with positive tumor AREG (n = 139) and those with negative AREG (n = 146) regarding the patient's sex, age, smoking status or PS (Table S5). However, a null tumor AREG expression was more frequent in patients with sarcomatoid or biphasic MPM than with epithelioid MPM ($P = .0081$, Cox model, Table S5).

Tumor AREG expression was associated with a better prognosis. The median OS of patients with positive tumor AREG was 22.2 months (95% CI [17.9-24.5]) vs 15.1 months (95% CI [13.2-16.8]) for patients with null AREG (adjusted [adj.] HR = 0.69, 95% CI [0.54-0.90], $P = .0052$) (Figure 1B). Similarly, median PFS was better in patients with positive AREG immunostaining: 8.8 months (95% CI [8.1-10.0]) vs 7.9 months (95% CI [6.6-8.6]) in patients with negative AREG expression (adj. HR = 0.71, 95% CI [0.55-0.90], $P = .0056$) (Figure 1C). An internal validation of this AREG H-score prognostic value was performed by bootstrap resampling in 1000 theoretical samples, which showed that AREG immunostaining significantly predicted both OS and PFS in 67.4% and 67.2% of the samples, respectively (Table S6).

In the whole trial's population (both arms mixed), the subcellular localization of AREG also significantly influenced patients' survival. Median OS of patients with cytosolic tumor AREG was 24.8 months (95% CI [19.6-35.6]) vs 15.9 months (95% CI [14.1-17.9]) when AREG was nuclear (HR = 0.61, 95% CI [0.44-0.84], $P = .003$) (Figure 1D). Median PFS of patients with cytosolic tumor AREG was 10.4 months (95% CI [8.4-13.3]) vs 8.2 months (95% CI [7.2-8.6]) when AREG was nuclear (Figure 1E, adj. HR = 0.60, 95% CI [0.40-0.88], $P = .009$).

Finally, while the frequency of the null tumor expression of AREG was lower in patients in the CisPem arm (45.1%) than in patients who received CisPem+Beva (57.3%) (Table S7, $P = .0382$, Cox model), AREG did not predict patients' relative survival in either treatment arm (*P*-value interaction test = .348 and .865 for OS and PFS, respectively).

### 3.2 | YAP transcriptional coactivator tumor expression was also associated with better prognosis in MPM patients from the MAPS trial

Since the transcriptional coactivator YAP governs AREG transcription,[5] we performed YAP immunohistochemistry on 306/448 MPM patients from the MAPS trial (Figure S2). The average YAP score was 220 ± 84.3, and the median was 240 [180-300]; only 4/306 cases showed negative staining with positive internal controls. Although YAP subcellular localization (nuclear or cytosolic, or both nuclear and cytosolic) (Figure S2B) did not influence OS or PFS (not shown), total YAP expression correlated with prognosis: the median OS of patients with intermediate YAP expression (180 ≤ H-score < 240) was 14.1 months (95% CI [12.1-17.9]) as compared to 19.6 months (95% CI [15.9-24.5]) for patients with high YAP expression (H-score ≥ 300, adj. HR = 0.69, 95% CI [0.51-0.94], $P = .02$) (Figure S2B). Similarly, the median PFS was significantly longer in the patients with high total YAP expression: 9.2 months (95% CI [8.2-10.6]) with YAP expression ≥300 vs 7.3 months (95% CI [6.4-8.6]) in patients with intermediate YAP expression (180 ≤ H-score < 240), adj. HR = 0.63, 95% CI [0.46-0.85], $P = .003$ (Figure S2C).

Like AREG expression, YAP staining failed to show any predictive value according to the treatment arm (bevacizumab-based or not) (not shown).

### 3.3 | Plasma AREG was rarely detected in MPM patients in the IFCT-GFPC-0701 MAPS trial

AREG was assayed in the plasma of 373/448 MPM patients (83.3%, Figure S1). While most MPM tumor specimens that were analyzed showed AREG staining, plasma AREG was detected in 42 of the 373 patients (11.26%). Since we previously found substantial VEGF concentrations in these same plasma samples,[21] we excluded widespread degradation of these plasma samples due to bad transport or cryopreservation conditions.

No correlation was found between plasma and tumor tissue AREG amounts ($r = .007$, $P = .91$). Plasma AREG concentrations were also not correlated with MPM patients' OS or PFS (not shown).

The fact that MPM tumors highly expressed AREG but that AREG was rarely found in the plasma of the same patient strongly suggests that the MPM cells failed to properly release AREG.

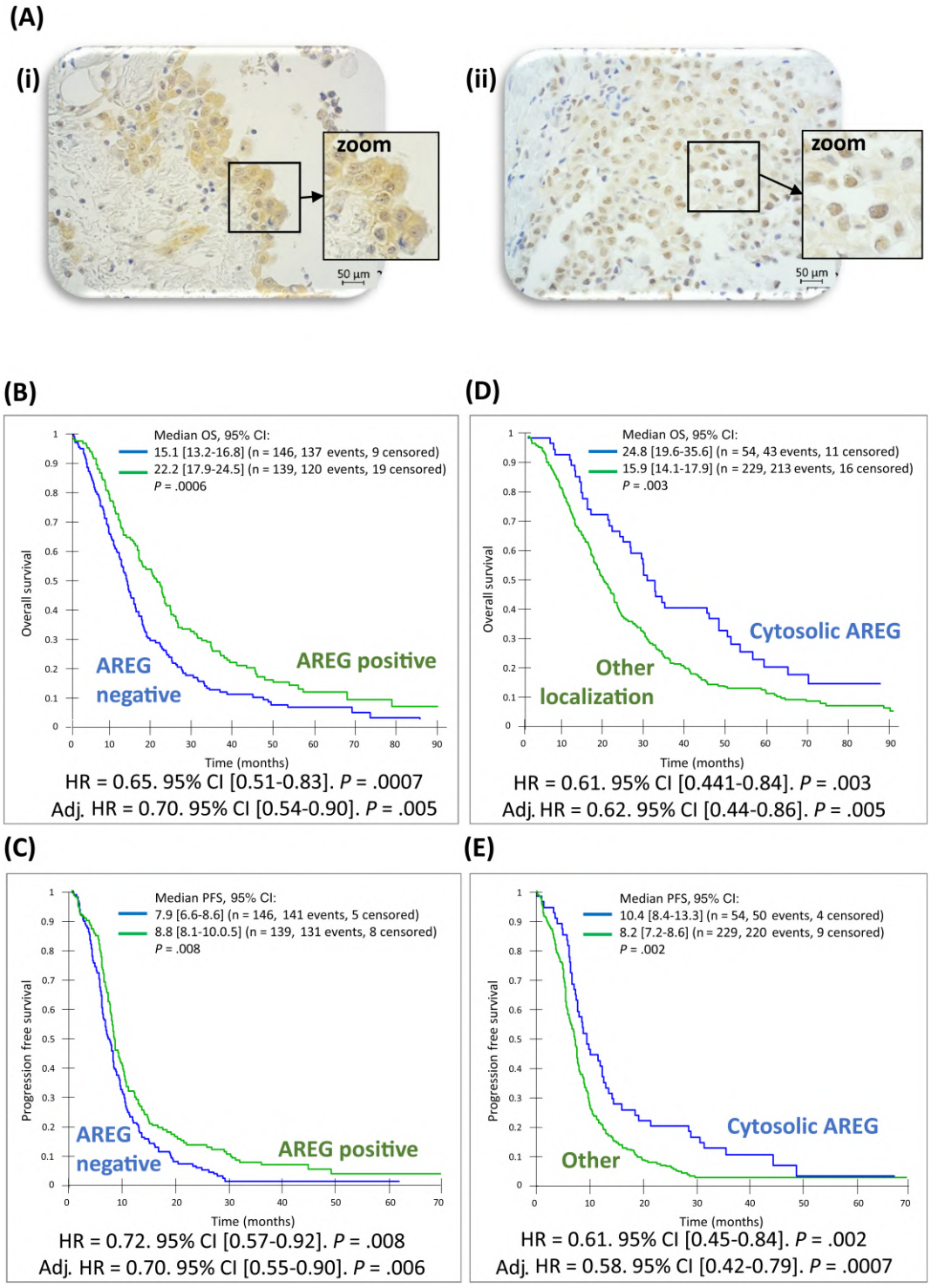


**FIGURE 1** Positive or cytosolic AREG predicted both better overall survival and progression-free survival in patients with malignant pleural mesothelioma. Representative cytosolic (Ai) or nuclear (Aii) AREG expression in an MPM specimen. Kaplan-Meier curve of overall survival (B and D) and progression-free survival (C and E) according to AREG expression (negative or positive, B and C) and subcellular localization (cytosolic or other, D and E). Adjustment for sex, age, histology, performance status, hemoglobin, white blood cells, platelet, smoking status and treatment arm [Color figure can be viewed at wileyonlinelibrary.com]

### 3.4 | MPM cell lines expressed low levels of AREG with predominant nuclear localization

Next, we investigated the AREG process in the human MPM cell lines H2452, H2052, MSTO-211H and H28. The T47D-ER+ breast cancer cell line was used as a positive control for normal AREG processing, as previously reported in the literature.[23] We measured the specific AREG expression at both the mRNA (Figure 2A) and protein level (Figure 2B,C) in each MPM cell line. However, the AREG levels were very low compared to the T47D cell line control, and there

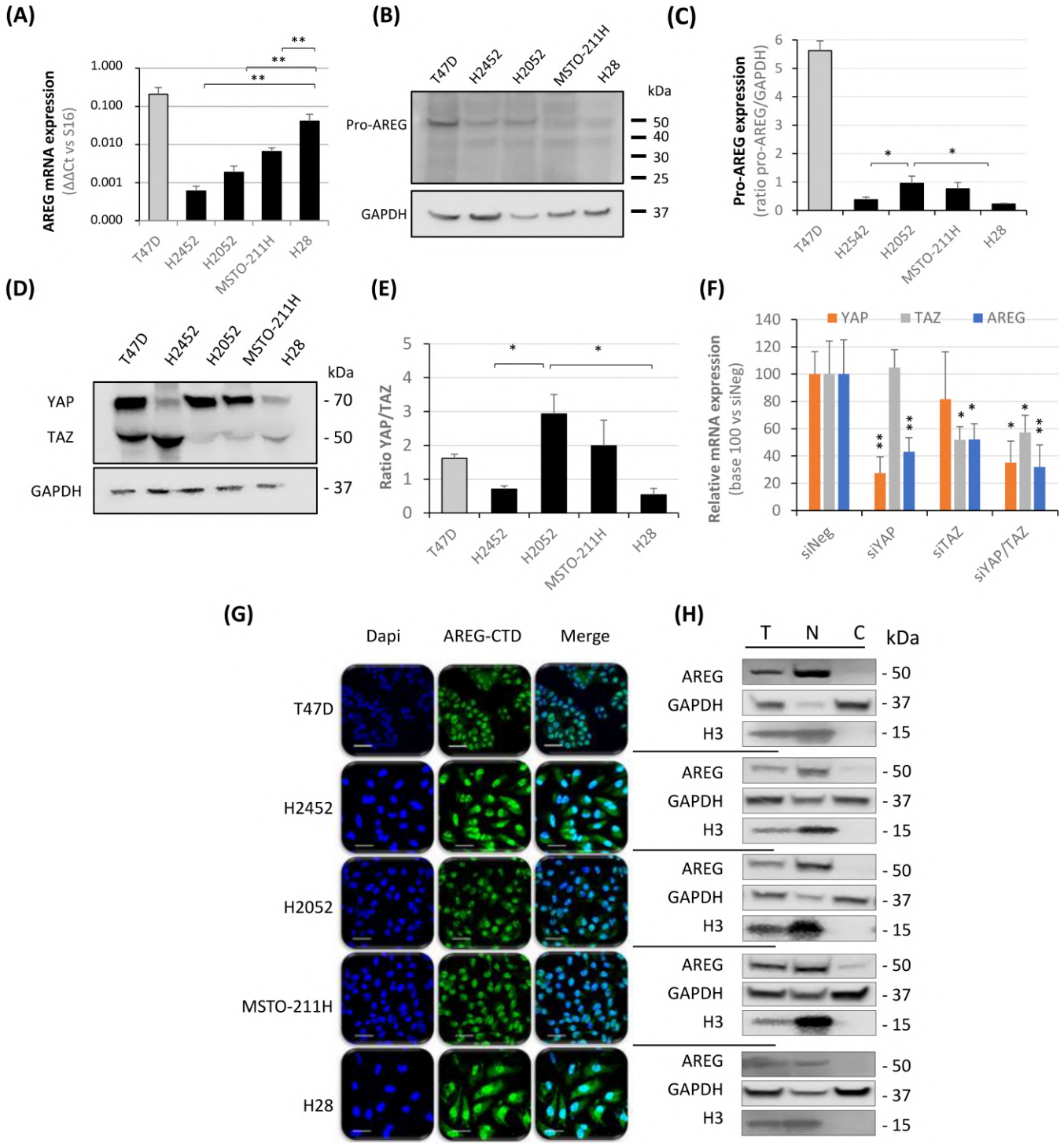


**FIGURE 2** AREG and YAP/TAZ expression in malignant pleural mesothelioma cell lines. AREG mRNA expression, as measured by RT-qPCR (A). Protein expression of AREG (B) and YAP/TAZ (#8418S Cell signaling) (D), as analyzed by western blot. Quantification of AREG (C) and YAP/TAZ ratio (E). (F) AREG expression in H28 cells after 48 hours of transfection with nonsilencing siRNA (siNeg), siYAP and/or siTAZ. Representative images (G) of AREG expression using an antibody against the AREG-CTD by immunofluorescence with DAPI for DNA. The scale bar represents 50 μm. (H) Representative western blot showing distribution of AREG, GAPDH and Histone H3 in Total (T), Nuclear-enriched (N) and Cytosolic (C) subcellular fraction (n = 3). (A), (C), (E) (F): results are mean ± SEM (n = 3), *$P < .05$, **$P < .01$ and ***$P < .001$; ANOVA followed by Dunnett's test [Color figure can be viewed at wileyonlinelibrary.com]

was no correlation between mRNA and protein levels. We hypothesized that AREG expression in MPM could be correlated with the status of the terminal effectors of the Hippo pathway, the transcriptional coactivators YAP and TAZ, since YAP and TAZ have previously been reported to contribute to AREG gene transcription.[4,24] Actually, MPM cell lines exhibited very divergent ratios of

YAP/TAZ: three expressed higher TAZ than YAP (Figure 2D,E) but evident relationship was found with AREG expression at the mRNA or the protein level and YAP/TAZ ratio. Silencing YAP and/or TAZ expression with siRNA significantly reduced AREG mRNA expression in H28 cell line (Figure 2F, YAP and TAZ extinction was validated at protein level by immunochemistry and western blot [Figure S3]) which exhibited the highest YAP/TAZ ratio, but the lowest expression level of YAP and TAZ. Such AREG mRNA downregulation was also evidenced in MSTO-211H cells transfected with siYAP or siTAZ, as well as in H2452 cells transfected with siTAZ, but conversely not in H2052 cell line (data not shown). Nuclear tumor cells YAP and total AREG staining in MPM patients from the IFCT-GFPC-0701 MAPS trial was only slightly, although if significantly correlated (correlation coefficient: .21; $P = .0004$). Taken together, these results suggest other currently unknown AREG gene transcription regulation mechanisms in MPM that possibly involve other transcription factors.

Remnant AREG C-terminal domain (AREG-CTD), during its shedding or recycling, and unshed pro-AREG exhibited different subcellular locations[25] with internalization and nuclear translocation of recycling pro-AREG, whereas after shedding, AREG-CTD was translocated to the lysosome.[26,27] We then examined the AREG protein location using a polyclonal goat antibody that recognizes both the unshed pro-AREG isoform and the AREG-CTD (Figure 2G). AREG staining was predominantly nuclear (for 61.0 ± 1.5% to 81.7 ± 3.4% of the staining, in T47D, H2452, H2052 and MSTO-211H cells, while it was more dispatched between both the nucleus [51.0 ± 3.6%] and cytoplasm in H28 cells). Subcellular fractionation experiments confirmed the accumulation of AREG in enriched nuclear fraction (N) compared to Total (T) or Cytosolic (C) fraction (Figure 2G,H). Thus, in our experimental conditions, high nuclear AREG staining might reflect a poor shedding activity and thus low secretion of sAREG.

Taken together, these results suggest that MPM cells weakly express AREG and exhibit a low AREG shedding activity.

### 3.5 | AREG depletion decreased 2D migration, invasion and growth without anchorage in human MPM cell lines

Forty-eight hours after silencing AREG in the human MPM cell lines using siRNAs (Figure S4, Table S1), compared to the siNeg-cells, AREG silencing significantly increased cell spread (Figure S3E, illustrated for MSTO-211H), decreased by almost twice the cell invasion capacity of the four MPM cell lines (Figure 3Ai-iv) and inhibited growth without adhesion of these MPM cell lines, excepted for H28, as shown by the decrease of both the colony number in agar (Figure 3Bi-iv) and the spheroid in suspension (Figure 3C, shown here for MSTO-211H) of AREG-depleted MPM cells, compared to the control (siNeg) MPM cells. AREG silencing also inhibited the 2D migration of H2452 and MSTO-211H cells (Figure S5A,B). To ensure the specificity of the cellular effects induced by AREG silencing, we also incubated MPM cells with exogenous AREG (20 ng/mL) for 24 hours before performing an invasion assay or when artificial "wound" was created for 2D migration. Exogenous AREG actually increased MPM cells' invasion in Matrigel or 2D migration and restored invasion and migration of the AREG-depleted MPM cells (Figures S5A and S6A: H2452, Figures S5B and S6B: MSTO-211H cells). As shown in Figure S5 (right panel), exogenous hAREG triggers the expected downstream signaling in MPM and AREG-depleted MPM cells as illustrated by the increase of both EGF-receptor and ERK phosphorylation 20 minutes after AREG addition.

Results from Figure 3 and Figures S5 and S6 demonstrate that AREG, even when weakly expressed, can influence invasion and growth without anchorage in human MPM cell lines.

### 3.6 | AREG depletion increased apoptosis and decreased the proliferation of human MPM cell lines

Furthermore, we observed that siAREG MPM cells were larger but less numerous than siNeg MPM cells 48 hours following cell transfection (Figure S4E, for MSTO-211H cells). Consistently, AREG depletion increased cell apoptosis, as assayed by measuring caspase-3/7 activities (Figure 4Ai-iv), while significantly lowering proliferation of H2452, H28 and H2052 cells (Figure 4Bii-iv); a strong trend toward such an effect was observed for the MSTO-211H cell line (Figure 4Bi).

Taken together, these results confirm that AREG can influence both cell proliferation and the apoptosis process in MPM cells. The decreased invasion and colony/spheroid formation of AREG-depleted MPM cells could be explained by such a concomitant decrease of proliferation and/or increase of cell death, as previously reported.[10]

### 3.7 | Most MPM cells exhibited defects in the shedding and release of AREG

Release of sAREG from the cell plasma membrane requires proteolytic processing that is achieved by a membrane-anchored metalloprotease TACE.[8] TACE is expressed at both mRNA (Figure S7A) and protein levels in the four MPM cell lines (Figure S7B,C), without significant differences across MPM cell lines or compared to the control T47D cell line. The TACE protein is predominantly expressed in the vicinity of and in the cell plasma membrane, as shown by punctate cytoplasmic staining (Figure S7D exemplified with H28 cell lines S7E). We evaluated the TACE shedding activity in MPM cells by measuring both cellular AREG and sAREG released into culture medium after 48 hours using a commercially available ELISA assay kit (Figure 5A). In the control T47D cell line, the amount of AREG recovered in the culture medium (216.2 ± 32.3 pg) was nearly three times higher than the amount of cellular AREG (77.54 ± 4.3 pg), which supports an active shedding of AREG. In contrast, for H2452, H2052 and MSTO-211H cells, levels of AREG that were measured in the cellular and culture medium were low, ranging from 1 to 4 pg, and they did not significantly differ in the cell compartment and medium. In such cell lines, the ratio of AREG measured in the cellular and culture medium was

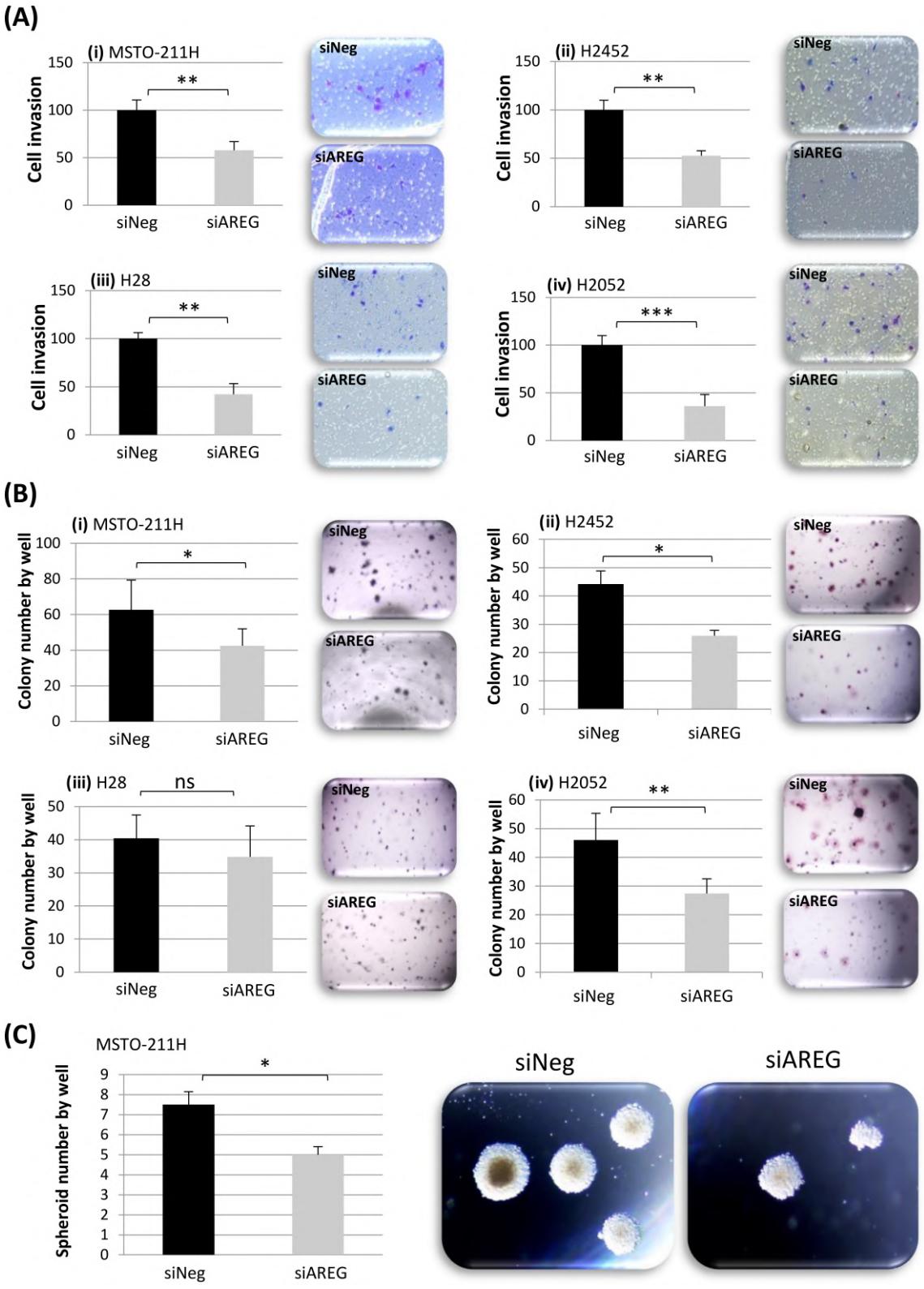


**FIGURE 3** AREG depletion decreased invasion and growth without anchorage of human malignant pleural mesothelioma cells. MSTO-221H, H2452, H28 and H2052 were transfected with nonsilencing siRNA (siNeg) or siAREG. Experiments were performed 48 hours after transfection. Invasion capacity of MSTO-221H (Ai), H2452 (Aii), H28 (Aiii) and H2052 (Aiv) on a BioCoat Matrigel Invasion Chamber, normalized to control cells (siNeg). Growth without anchorage of MSTO-221H (Bi), H2452 (Bii), H28 (Biii) and H2052 (Biv) on soft agar following 21 days of culture. Histograms represent colony number per well. Growth without anchorage of MSTO-221H cultured in suspension (Nucleon Sphera Microplates, Thermo Fisher Scientific). Histograms represent spheroid number per well (C). Scale bar represents 80 μm. Error bars indicate SEM (n = 3, *$P$ < .05, **$P$ < .01 and ***$P$ < .001; ANOVA followed by Dunnett's test) [Color figure can be viewed at wileyonlinelibrary.com]

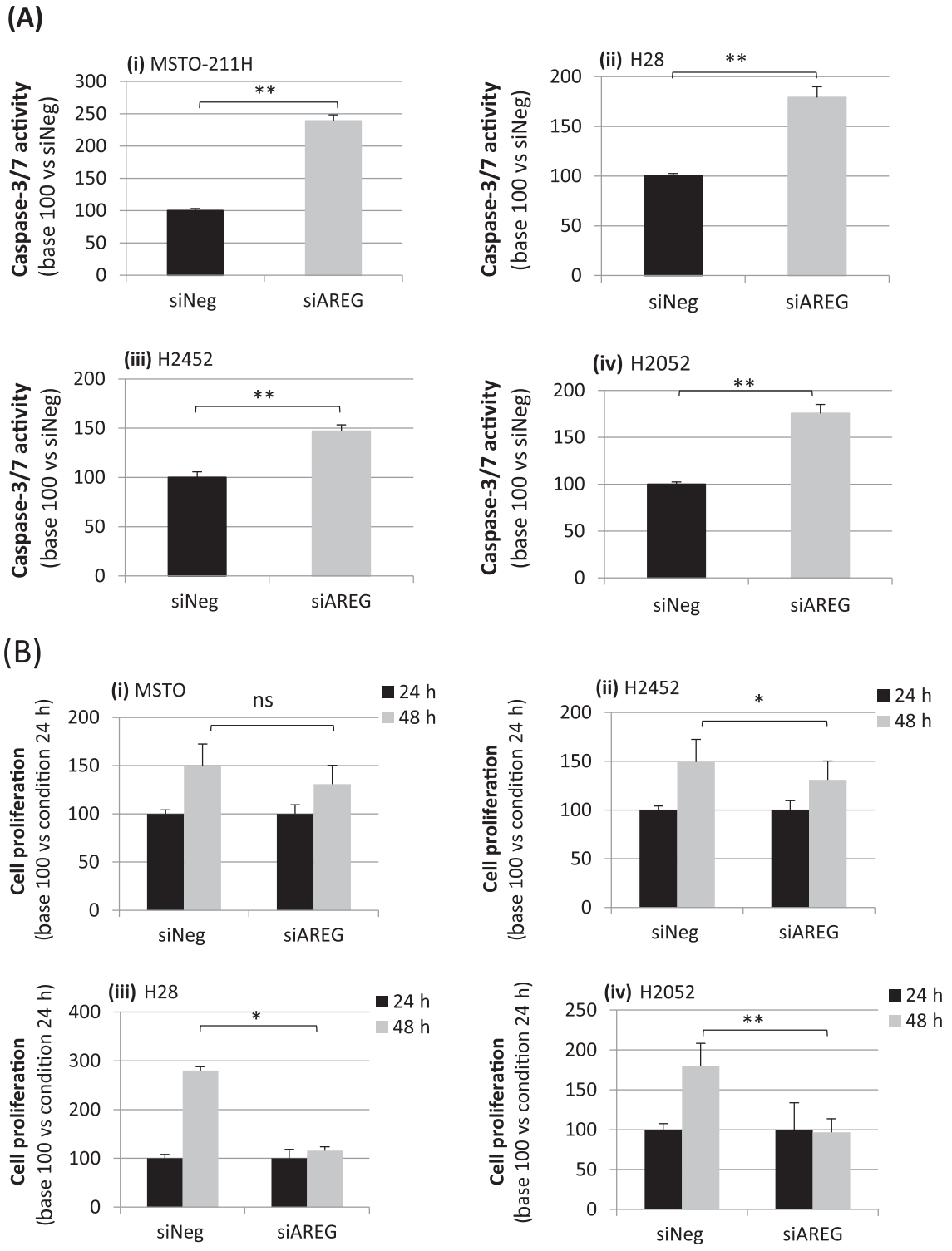


**FIGURE 4** AREG depletion decreased proliferation and increased apoptosis of human malignant pleural mesothelioma cells. MSTO-221H, H2452, H28 and H2052 were transfected with nonsilencing siRNA (siNeg) or siAREG. Experiments were performed 48 hours after transfection. Caspase-3/7 activity measurements for MSTO-221H (Ai), H2452 (Aii), H28 (Aiii) and H2052 (Aiv). BrdU incorporation in MSTO-221H (Bi), H2452 (Bii), H28 (Biii) and H2052 (Biv) 24 or 48 hours following the addition of BrdU. Error bars indicate SEM (n ≥ 3) of $^{*}P < .05$, $^{**}P < .01$ and $^{***}P < .001$, using an ANOVA test followed by Dunnett's test

only 0.6-, 1.6- and 2.8-fold for H2452, H2052 and MSTO-211H, respectively. H28 was the only cell line that exhibited a significant amount of cell-associated AREG (69.6 ± 15.1 pg), and sAREG was detected in the culture medium (459.7 ± 7.7 pg). This represents a 6.9-fold higher amount of cellular AREG, which indicates active shedding of AREG in the cell culture medium for this cell line.

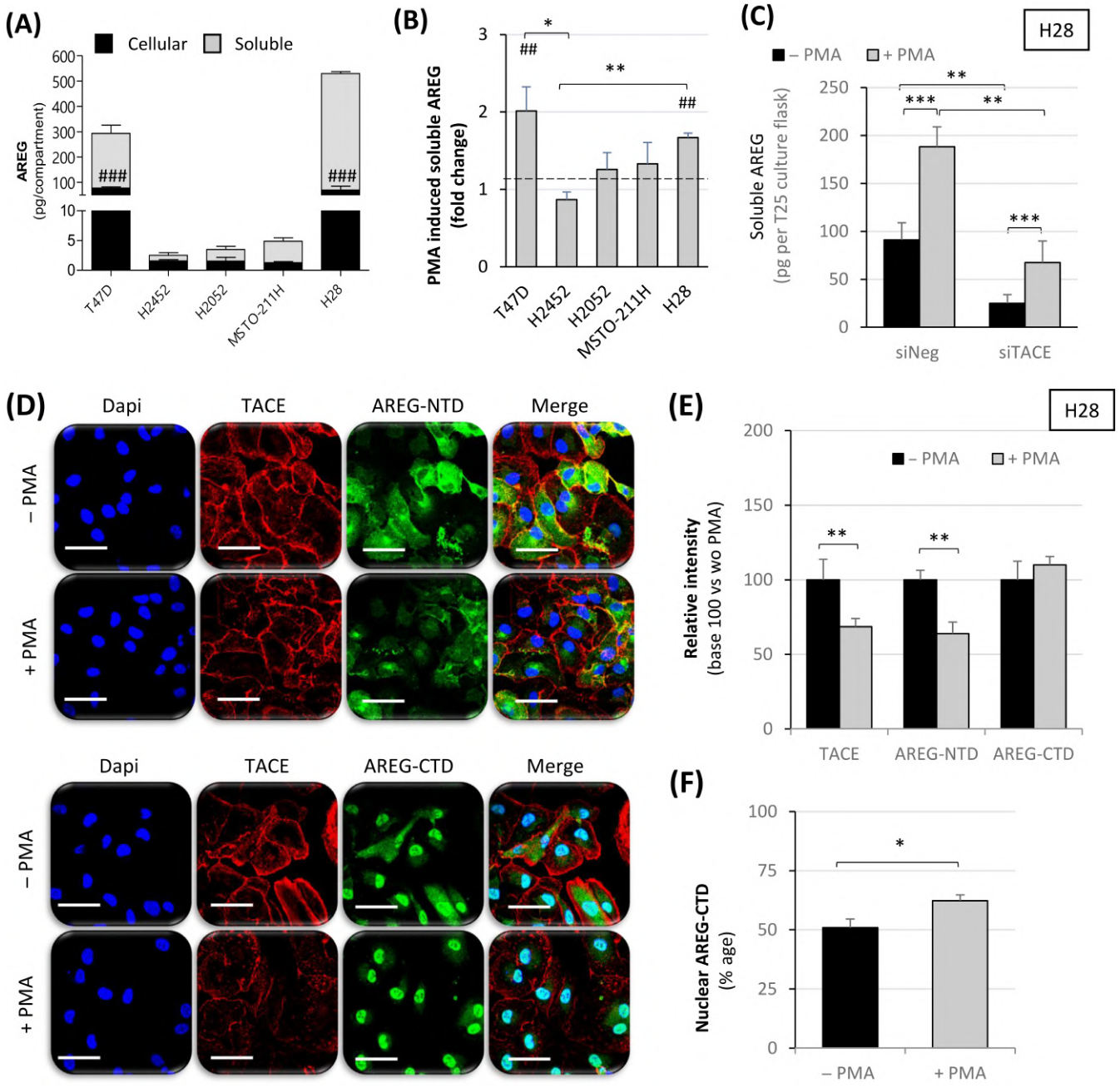


**FIGURE 5** Malignant pleural mesothelioma cell lines exhibited low AREG shedding activity. Cellular and soluble AREG were measured after 48 hours of cell culture by ELISA assay in the culture medium and in the cellular layer, respectively (A). The soluble AREG release was measured in the culture medium of cells that had been stimulated or not with PMA (25 ng/mL) for 3 hours (B): $^{*}P < .05$, $^{**}P < .01$ and $^{***}P < .001$, using an ANOVA test followed by a Tukey test (n = 3); $^{\#\#}P < .01$ and $^{\#\#\#}P < .01$, using the *t*-test by comparing cellular vs soluble AREG for (A) or PMA-treated vs untreated AREG for (B). (C): Soluble AREG was quantified by ELISA in H28 cells transfected with siTACE for 48 hours and stimulated with PMA (25 ng/mL) for 3 hours, after the culture medium had been refreshed: $^{*}P < .05$, $^{**}P < .01$ and $^{***}P < .001$, using an ANOVA test followed by a Tukey test (n = 4). H28 cell expression of TACE and AREG following PMA stimulation (30 minutes) was estimated by immunohistochemistry (D) and quantified using Image J software (E). For AREG, the antibody against AREG-NTD (upper panel) or AREG-CTD (lower panel) was used. The percentage of AREG-CTD nuclear staining was then quantified: $^{*}P < .05$, $^{**}P < .01$, using a Student's *t*-test (n = 3) (F) [Color figure can be viewed at wileyonlinelibrary.com]

PMA was shown to increase AREG shedding (peptide cleavage) in a TACE-dependent manner.[28] Next, we treated MPM cells for 3 hours with 25 ng/mL of PMA, which actually led to a significant increase of sAREG, as measured in the medium for both the H28 and T47D cell lines (2.0 ± 0.3 and 1.7 ± 0.1-fold, respectively), compared to basal shedding (Figure 5B). At the same time, no modification of cellular AREG content was noticed within these cells (not shown), suggesting that the increase of sAREG in H28 and T47D upon PMA treatment was not the consequence of AREG increased synthesis, but rather the result of TACE-induced AREG cleavage. No increase of sAREG upon

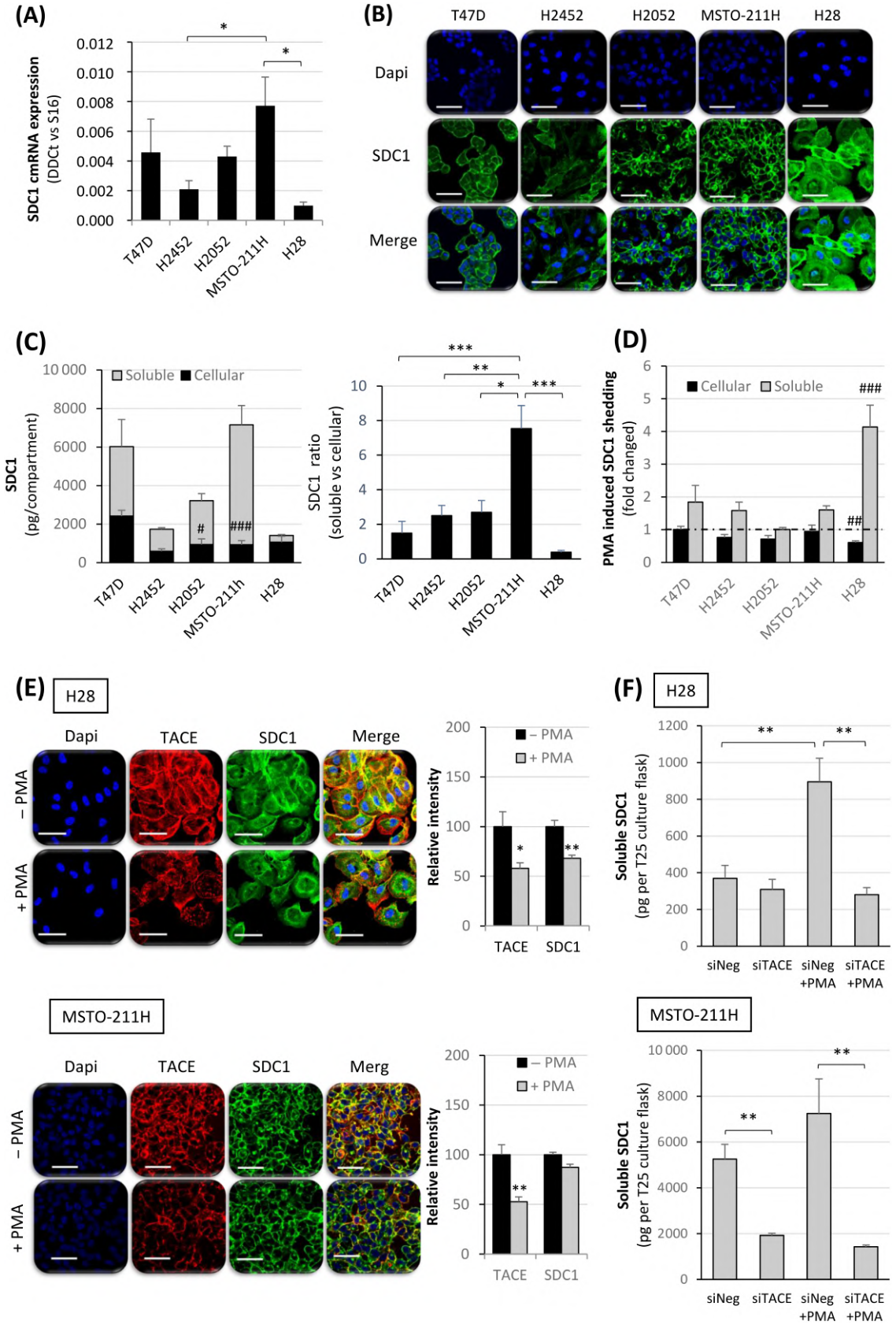


**FIGURE 6** Legend on next page.

PMA stimulation was observed in the other MPM cell lines, again supporting a defect in AREG shedding (Figure 5B).

Transient RNAi-mediated silencing of TACE, which significantly decreased mRNA (−70.6 ± 8.4%) and protein expression (−45.5 ± 4.5%) (Figure S7F-H), drastically reduced PMA-induced AREG shedding and its release in the H28 cell line (Figure 5C). Activation of AREG shedding by PMA (25 pg/mL for 30 minutes) was confirmed in these cells by immunocytochemistry (Figure 5D). For the upper panel, a polyclonal goat IgG raised against the N-terminal domain of AREG (Val107-Lys184, R&D systems), corresponding to the mature sAREG and called "AREG-NTD," was used. For the lower panel, the AREG-CTD antibody-recognizing cellular AREG was assayed. A coimmunostaining was also performed with an anti-TACE antibody for both. Quantification of the different staining showed a significant decrease of TACE (−31.4 ± 5.4%) and AREG-NTD (−36.1 ± 7.8%) contents following PMA stimulation (Figure 5E). In contrast, when using the AREG-CTD antibody, no variation of total signal intensity was measured after PMA stimulation, while a faint but significant increase of nuclear staining was observed (Figure 5F).

These results revealed that TACE activity and sAREG release are very low in some MPM cell lines, while PMA stimulation of TACE activity seems to be restricted to some specific MPM cells, such as the H28 cell line.

Then, we wondered whether the loss of AREG ectodomain shedding in MPM cells could be related to mutations in the catalytic (C225Y) and cysteine rich/disintegrin (C600Y) domains of TACE, as reported in Chinese hamster ovary (CHO) sublines.[29] Direct sequencing did not reveal such mutations in MPM cell lines (Figure S8). Accordingly, loss of AREG shedding in MPM cell lines could not be explained by these point mutations of the *TACE* gene.

### 3.8 | TACE cleaved AREG and its coreceptor syndecan-1 differentially in MPM cell lines

Syndecan-1 (SDC1, also known as CD138) is a transmembrane heparan sulfate proteoglycan and a coreceptor of the sAREG, which facilitates its binding to EGFR.[30] SDC1 is also cleaved by membrane-associated TACE.[28] MPM cell lines express SDC1 at both mRNA and protein levels (Figure 6A,B).[31] Thus, using the same approach as for the AREG shedding assay, we used ELISA to quantify cell-associated SDC1 and shedded ectodomain that was released into the medium (Figure 6C). We found a comparable amount of cell-associated SDC1 in the MPM cell lines. In contrast, the level of soluble SDC1 was significantly higher in the culture medium of MSTO-211H cells than in the culture medium of other MPM cell lines. Soluble-cellular ratio was 7.5 ± 1.3 in the MSTO-211H cell line, 2.5 ± 0.6 in H2452 and 2.6 ± 07 in H2052. In the H28 cell line, in which a constitutive AREG shedding had been measured (Figure 5A), a very low basal SDC1 shedding was found, with a soluble-cellular ratio below 1, at 0.4 ± 0.1. However, H28 was the only cell line that was able to respond to PMA stimulation, as illustrated by a decrease in cell-associated SDC1 content, with a concurrent 4.1 ± 0.6-fold increase of soluble SDC1, which was measured in the culture medium (Figure 6D). Additionally, a decrease of cellular TACE and SDC1 staining was also demonstrated after 30 minutes of PMA stimulation in the H28 cells (Figure 6E). This SDC1 protein content variation was not found for MSTO-211H by either ELISA (Figure 6D) or immunocytochemistry (Figure 6E). However, in both cell lines, a decrease of cellular TACE staining following PMA treatment was observed, which aligns with previous data showing a downregulation of TACE following PMA treatment and occurring via the internalization and degradation of TACE molecules.[32] While TACE silencing significantly reduced constitutive SDC1 shedding on MSTO-211H cells, this treatment was ineffective in H28, in which the basal SDC1 cleavage was low (Figure 6F). Nonetheless, the PMA-induced SDC1 shedding that was observed in the H28 cell line was totally reversed after the TACE knockdown (Figure 6F).

These data showed that TACE is also responsible for basal or PMA-induced cleavage of SDC1 in MPM cells, but that the constitutive SDC1 or AREG shedding could differ from one MPM cell line to the other, while PMA-induced protein proteolytic activation still depends on TACE in all cell lines. Such findings could account for the observed variations in the AREG cytosolic content of the MPM samples and could support the prognostic role of unshed, cytosolic AREG in MPM.

## 4 | DISCUSSION

AREG overexpression was previously observed in MPM cells, compared to normal pleural mesothelial cells,[18] but we here provide data reinforcing that tumor AREG could also be used as a prognostic marker for MPM patients. We confirmed that 64.3% of MPM patients highly expressed tumor AREG and that this expression is more frequent in patients with the epithelioid histological subtype, such patients being known to have a better prognosis with higher chemo-sensitivity.

**FIGURE 6** SDC1 shedding activity in malignant pleural mesothelioma cell lines. Expression of SDC1 mRNA in MPM cell lines and T47D: $^{*}P < .05$, using an ANOVA test followed by a Tukey test (n = 4) (A). SDC1 was visualized by immunocytochemistry after staining of the nuclei with DAPI. The scale bar represents 50 μm (B). Cellular and soluble SDC1 were measured by ELISA assay in the culture medium and in the cellular layer, respectively, for each cell line after 48 hours of culture (left panel). The ratio of soluble to cellular amounts of SDC1 was then calculated (right panel) (n = 3): $^{\#}P < .05$ and $^{\#\#\#}P < .01$, using a *t*-test by comparing cellular vs soluble SDC1; $^{*}P < .05$, $^{**}P < .01$ and $^{***}P < .001$, using an ANOVA test followed by a Tukey test (C). Soluble and cell-associated SDC1 were measured by ELISA 3 hours after PMA stimulation (n = 3): $^{\#\#}P < .01$ and $^{\#\#\#}P < .01$, using a Student's *t*-test by comparing PMA-treated and untreated conditions (D). Expression of TACE and SDC1 in the H28 and MSTO-211H cell lines following PMA stimulation (30 minutes, 25 pg/mL): $^{*}P < .05$ and $^{**}P < .01$, using a Student's *t*-test by comparing PMA-treated vs untreated conditions (n = 3) (E). H28 and MSTO-211H cells were transfected with siNeg or siTACE (20 nM), some of which were stimulated with PMA (25 pg/mL for 3 hours), and soluble SDC1 was measured in the culture medium by ELISA: $^{**}P < .01$, using an ANOVA test followed by a Tukey test (n = 3) (F) [Color figure can be viewed at wileyonlinelibrary.com]

We also reported that cytosolic AREG expression predicted longer OS and PFS. Finally, we found that this prognostic value could be sustained by default AREG posttranslational processing and a defect in AREG release in human MPM cells.

AREG can either stimulate or inhibit the growth of various normal and cancer cell lines.[33] AREG is mostly described as an oncogenic factor: It is indeed found to be overexpressed[34] and associated with reduced OS[35] in the most common human epithelial carcinomas, for example predicting metastastic ability in colorectal cancer.[15] In advanced NSCLC patients, AREG tumor cell overexpression[36] and high plasma levels of AREG[37] also significantly correlated with poor response rates to the EGFR inhibitors gefitinib and cetuximab.[14] Conversely, high AREG expression was associated with longer OS and PFS in colorectal cancer.[38,39] Our findings regarding high AREG expression in MPM cells were thus consistent with existing literature. This high AREG expression in MPM cells could be sustained by the frequently reported abnormal YAP activity in these cells. Actually, recent studies have shown an activation of YAP due to epigenetic inactivation of some upstream Hippo pathway components in MPM patients.[2] AREG belongs to the wide array of YAP-targeted genes.[5] Consistently with the frequent expression of AREG by MPM cells, we found frequent and high expression of YAP. As with AREG, YAP global expression (whatever the subcell compartment) also predicted longer OS and PFS in MPM patients accrued in the MAPS trial, regardless of the treatment arm (containing anti-VEGF bevacizumab or not).

As previously discussed, during its posttranslational "cycle," AREG can have successive subcellular localizations.[25,40] Such different subcellular localizations are assigned to specific cell types with various consequences, according to different cancer types. For example, in high-grade prostatic intraepithelial neoplasia and adenocarcinoma, AREG nuclear staining was predominantly observed in benign epithelium, whereas cytoplasmic or nuclear and cytoplasmic staining was observed in tumor cells.[41] In gastric cancer, the AREG nuclear translocation contributes to chemoresistance.[42] Accordingly, AREG is a bifunctional modulator that can either stimulate or inhibit the growth of lung cancer cells, depending on the biological background.[43] In our series of MPM patients, high AREG cytosolic expression was a factor of better prognosis, with significant increases of both median OS and PFS, compared to low cytosolic AREG. Several explanations could account for this effect: Either a lower nuclear localization could counteract the role played by nuclear AREG in chemoresistance, or the defect in the membrane pro-AREG shedding could reduce the autocrine or paracrine roles of sAREG, particularly in terms of inducing activation of EGFR or VEGFR-2, with the activation of their downstream key signaling pathways, while uncleaved pro-AREG and AREG-CTD could lead to alternative intracellular signaling.[27,44]

Despite high AREG tumor expression, plasma AREG was only detected in 11.26% of patients whose blood samples were collected, and this blood AREG failed to correlate with survival or with cell AREG expression. To reconcile this apparent discrepancy, we assumed that mesothelial tumor cells could present specific defects of AREG release. Surprisingly, by characterizing AREG expression in MPM cells, we report no correlation between the AREG mRNA level and the mature AREG protein content. The antibody used recognizes the EGF-like domain of the mature AREG protein, a domain which could be secreted after proteolytic cleavage. It might thus explain a loss of the AREG signal associated with the cells and the observed apparent difference between mRNA and protein contents. Such hypothesis is in line with the high level of AREG mRNA and low AREG protein contents in H28 cells, the only MPM cells we used that were shown to secrete AREG. Moreover, this lack of correlation was already reported in lung cancer[45] or in astrocytoma[46] by other authors. This suggests a complex multifactorial mechanism for transcriptional and post translational regulation of AREG processing, which might be differentially regulated depending on cell type and physiological context.

By examining the AREG protein subcellular localization in the MPM cell lines, we measured a very low level of AREG in the MPM cell culture medium, and pro-AREG was predominantly nuclear, as described elsewhere.[27,42,44] This is consistent with the observation that pro-AREG, when not cleaved at the plasma membrane, could translocate to the inner nuclear membrane, where it binds to A-type lamin; this results in heterochromatin formation that leads to the suppression of global transcription,[44] yet another established physiological role for AREG.

MPM is not the only cancer that presents such an AREG release defect. Glioblastoma with wild-type isocitrate dehydrogenase (IDH) also exhibits elevated AREG mRNA expression, but with a reduced AREG protein level, compared to grade II and grade III (IDH-mutated) astrocytomas.[46] Thus, glioblastoma is another cancer type with improved PFS using bevacizumab.[47]

The fact that AREG fails to be properly released in MPM cells does not mean that MPM cells are insensitive to AREG stimulation. Consistently, AREG silencing decreases MPM cell lines' invasion as well as colony and spheroid formation, while exogenous AREG restores invasion capacity and shows a prosurvival effect. These results coincide with the functional role of AREG in several aspects of tumorigenesis, including self-sufficiency in the generation of growth signals, unlimited replicative potential,[48] tissue invasion and metastasis,[15,16,49] decrease in adherent junctions,[49] promotion of anchorage-independent cell growth,[50] and extracellular matrix remodeling.[17,51] Finally, AREG, which did not induce migration in normal mesothelial cells, stimulates the chemotaxis and/or chemokinesis of various MPM cell lines.[17]

We also provide some insights into why MPM cells trap AREG by showing that TACE, the enzyme responsible for its shedding, exhibits weak activity in most of the MPM cell lines that were studied. Furthermore, only H28 cells release more AREG following stimulation by PMA. MPM cells exhibited no mutation in the catalytic TACE domain, such as the mutations described in CHO cells,[29] and TACE activity was conserved in MPM cells, since the TACE substrate SDC1 was efficiently cleaved in all but one of the MPM cell lines that we tested. This exception, which was the H28 cell line, was found to be able to cleave SDC1 in a TACE-dependent way upon PMA treatment, since the PMA action was counteracted by RNAi-mediated knockdown of TACE. Further investigations are thus needed to discover how TACE selectively cleaves its different targets according to the cellular context.

In conclusion, we propose that cytosolic AREG tumor expression, as determined by immunohistochemistry, could serve as a prognosis biomarker to identify MPM patients with better prognosis.

Although the basic mechanism that sustains the prognostic influence of AREG remains elusive, a defect in AREG processing was observed in most of the MPM cells that were studied. Whether patients with high cytosolic AREG expression represent a subset that could specifically benefit from the emerging new standard of MPM treatment, which relies on combination immunotherapy (anti-PD-1 and anti-CTLA-4), remains to be established. Drug screening that identifies compounds altering AREG processing could also represent a new therapeutic path for tumors with normal AREG expression.

## ACKNOWLEDGEMENT

The authors thank the CMABio3 platform.

## CONFLICT OF INTEREST

Valérie Gounant reports personal fees from MSD, Chugai, Novartis and Boehringer; personal fees and nonfinancial support from Astra Zeneca, BMS, Takeda and Pfizer; grants, personal fees and nonfinancial support from Roche, all outside the submitted work. Hervé Lena is a Roche board expert, but outside the submitted work. Denis Moro-Sibilot reports lectures for BMS, MSD, Roche, Astrazeneca, research grant from BMS, MSD, Roche, Astrazeneca and consulting for BMS, MSD, Roche and Astrazeneca, all outside the submitted work. Arnaud Sherpereel participated to expert's boards with BMS, MSD, Astrazeneca and Roche. His institution (CHU of Lille, France) received funding for research studies and clinical trials from BMS, Astrazeneca, MSD and Roche, all outside the submitted work. Gérard Zalcman is the principal investigator of the MAPS trial sponsored by the French Intergroup (IFCT) with a research grant to IFCT for funding ancillary studies from Roche, France. The other authors declare that they have no conflict of interest.

## AUTHOR CONTRIBUTIONS

*Conception and design*: Jérôme Levallet, Gérard Zalcman, Guénaëlle Levallet. *Development of methodology*: Guénaëlle Levallet, Elodie Maille, Jérôme Levallet. *Acquisition of data (provided animals, acquired and managed patients, provided facilities, etc)*: Guénaëlle Levallet, Elodie Maille, Fatéméh Dubois, Jérôme Levallet, Martine Antoine, Claire Danel, Julien Mazieres, Jacques Margery, Laurent Greillier, Valérie Gounant, Denis Moro-Sibilot, Olivier Molinier, Hervé Léna, Isabelle Monnet, Emmanuel Bergot, Arnaud Sherpereel, Gérard Zalcman. *Analysis and interpretation of data (eg, statistical analysis, biostatistics, computational analysis)*: Guénaëlle Levallet, Gérard Zalcman, Jérôme Levallet, Alexandra Langlais, Christian Creveuil. *Writing, review and/or revision of the manuscript*: Jérôme Levallet, Elodie Maille, Gérard Zalcman, Guénaëlle Levallet. *Administrative, technical or material support (ie, reporting or organizing data, constructing databases)*: Elodie Maille, Alexandra Langlais, Christian Creveuil, Franck Morin. *Study supervision*: Gérard Zalcman, Guénaëlle Levallet. The work reported in the study has been performed by the authors, unless clearly specified in the text.

## DATA AVAILABILITY STATEMENT

All data are stored at the IFCT center and can be made available upon request.

## ETHICS STATEMENT

Specific informed consent was obtained for the biological studies (Bio-MAPS), and the trial was approved by the appropriate ethics committee (CPP Ref 2007-20 Nord-Ouest III, France).

## ORCID

*Guénaëlle Levallet* https://orcid.org/0000-0001-7772-0581

## REFERENCES

1. Bueno R, Stawiski EW, Goldstein LD, et al. Comprehensive genomic analysis of malignant pleural mesothelioma identifies recurrent mutations, gene fusions and splicing alterations. *Nat Genet*. 2016;48:407-416.
2. Tranchant R, Quetel L, Tallet A, et al. Co-occurring mutations of tumor suppressor genes, LATS2 and NF2, in malignant pleural mesothelioma. *Clin Cancer Res*. 2017;23:3191-3202.
3. Maille E, Brosseau S, Hanoux V, et al. MST1/hippo promoter gene methylation predicts poor survival in patients with malignant pleural mesothelioma in the IFCT-GFPC-0701 MAPS phase 3 trial. *Br J Cancer*. 2019;120:387-397.
4. Wagner JC, Sleggs CA, Marchand P. Diffuse pleural mesothelioma and asbestos exposure in the North Western Cape Province. *Br J Ind Med*. 1960;17:260-271.
5. Park JH, Shin JE, Park HW. The role of hippo pathway in cancer stem cell biology. *Mol Cells*. 2018;41:83-92.
6. Zhang J, Ji JY, Yu M, et al. YAP-dependent induction of amphiregulin identifies a non-cell-autonomous component of the hippo pathway. *Nat Cell Biol*. 2009;11:1444-1450.
7. Plowman GD, Green JM, McDonald VL, et al. The amphiregulin gene encodes a novel epidermal growth factor-related protein with tumor-inhibitory activity. *Mol Cell Biol*. 1990;10:1969-1981.
8. Duffy MJ, McKiernan E, O'Donovan N, McGowan PM. Role of ADAMs in cancer formation and progression. *Clin Cancer Res*. 2009;15:1140-1144.
9. Schuger L, Skubitz AP, Gilbride K, Mandel R, He L. Laminin and heparan sulfate proteoglycan mediate epithelial cell polarization in organotypic cultures of embryonic lung cells: evidence implicating involvement of the inner globular region of laminin beta 1 chain and the heparan sulfate groups of heparan sulfate proteoglycan. *Dev Biol*. 1996;179:264-273.
10. Hurbin A, Dubrez L, Coll JL, Favrot MC. Inhibition of apoptosis by amphiregulin via an insulin-like growth factor-1 receptor-dependent pathway in non-small cell lung cancer cell lines. *J Biol Chem*. 2002;277:49127-49133.
11. Qi CF, Liscia DS, Normanno N, et al. Expression of transforming growth factor alpha, amphiregulin and cripto-1 in human breast carcinomas. *Br J Cancer*. 1994;69:903-910.
12. Tinhofer I, Klinghammer K, Weichert W, et al. Expression of amphiregulin and EGFRvIII affect outcome of patients with squamous cell carcinoma of the head and neck receiving cetuximab-docetaxel treatment. *Clin Cancer*. 2011;17:5197-5204.
13. Gao J, Ulekleiv CH, Halstensen TS. Epidermal growth factor (EGF) receptor-ligand based molecular staging predicts prognosis in head and neck squamous cell carcinoma partly due to deregulated EGF induced amphiregulin expression. *J Exp Clin Cancer Res*. 2016;35:151-163.
14. Ishikawa N, Daigo Y, Takano A, et al. Increases of amphiregulin and transforming growth factor-α in serum as predictors of poor response to gefitinib among patients with advanced non-small cell lung cancers. *Cancer Res*. 2005;65:9176-9184.
15. Yamada M, Ichikawa Y, Yamagishi S, et al. Amphiregulin is a promising prognostic marker for liver metastases of colorectal cancer. *Clin Cancer Res*. 2008;14:2351-2356.
16. Chayangsu C, Sriuranpong V. Serum amphiregulin in colorectal carcinoma and the correlation with liver metastasis. *J Clin Oncol*. 2016;34:e15078.

17. Liu Z, Klominek J. Chemotaxis and chemokinesis of malignant mesothelioma cells to multiple growth factors. *Anticancer Res*. 2004;24:1625-1630.
18. Cesario A, Catassi A, Festi L, et al. Farnesyltransferase inhibitors and human malignant pleural mesothelioma: a first-step comparative translational study. *Clin Cancer Res*. 2005;11:2026-2037.
19. Marino D, Angehrn Y, Klein S, et al. Activation of the epidermal growth factor receptor promotes lymphangiogenesis in the skin. *J Dermatol Sci*. 2013;71:184-194.
20. Yuan W, Xu W, Li Y, et al. TAZ sensitizes EGFR wild-type non-small-cell lung cancer to gefitinib by promoting amphiregulin transcription. *Cell Death Dis*. 2019;10:283-294.
21. Zalcman G, Mazieres J, Margery J, et al. Bevacizumab for newly diagnosed pleural mesothelioma in the mesothelioma avastin cisplatin pemetrexed study (MAPS): a randomised, controlled, open-label, phase 3 trial. *Lancet*. 2016;387:1405-1414.
22. Dubois F, Keller M, Calvayrac O, et al. RASSF1A suppresses the invasion and metastatic potential of human non-small cell lung cancer cells by inhibiting YAP activation through the GEF-H1/RhoB pathway. *Cancer Res*. 2016;76:1627-1640.
23. Peterson EA, Jenkins EC, Lofgren KA, et al. Amphiregulin is a critical downstream effector of estrogen signaling in ERα-positive breast cancer. *Cancer Res*. 2015;75:4830-4838.
24. Yang N, Morrison CD, Liu P, et al. TAZ induces growth factor-independent proliferation through activation of EGFR ligand amphiregulin. *Cell Cycle*. 2012;11:2922-2930.
25. Tokumaru S, Higashiyama S, Endo T, et al. Ectodomain shedding of epidermal growth factor receptor ligands is required for keratinocyte migration in cutaneous wound healing. *J Cell Biol*. 2000;151:209-220.
26. Berasain C, Avila MA. Amphiregulin. *Semin Cell Dev Biol*. 2014;28:31-41.
27. Stoll SW, Stuart PE, Lambert S, et al. Membrane-tethered intracellular domain of amphiregulin promotes keratinocyte proliferation. *J Invest Dermatol*. 2016;136:444-452.
28. Pruessmeyer J, Martin C, Hess FM, et al. A disintegrin and metalloproteinase 17 (ADAM17) mediates inflammation-induced shedding of syndecan-1 and -4 by lung epithelial cells. *J Biol Chem*. 2010;285:555-564.
29. Li X, Fan H. Loss of ectodomain shedding due to mutations in the metalloprotease and cysteine-rich/disintegrin domains of the tumor necrosis factor-alpha converting enzyme (TACE). *J Biol Chem*. 2010;279:27365-27375.
30. Mahtouk K, Cremer FW, Rème T, et al. Heparan sulphate proteoglycans are essential for the myeloma cell growth activity of EGF-family ligands in multiple myeloma. *Oncogene*. 2006;25:7180-7191.
31. Kumar-Singh S, Jacobs W, Dhaene K, et al. Syndecan-1 expression in malignant mesothelioma: correlation with cell differentiation, WT1 expression, and clinical outcome. *J Pathol*. 1998;186:300-305.
32. Doedens JR, Mahimkar RM, Black RA. TACE/ADAM-17 enzymatic activity is increased in response to cellular stimulation. *Biochem Biophys Res Commun*. 2003;308:331-338.
33. Shoyab M, McDonald VL, Bradley JG, Todaro GJ. Amphiregulin: a bifunctional growth-modulating glycoprotein produced by the phorbol 12-myristate 13-acetate-treated human breast adenocarcinoma cell line MCF-7. *Proc Natl Acad Sci USA*. 1988;85:6528-6532.
34. Busser B, Sancey L, Josserand V, et al. Amphiregulin promotes BAX inhibition and resistance to gefitinib in non-small-cell lung cancers. *Mol Ther*. 2010;18:528-535.
35. Wang L, Wu H, Wang L, et al. Expression of amphiregulin predicts poor outcome in patients with pancreatic ductal adenocarcinoma. *Diagn Pathol*. 2016;11:60-68.
36. Fontanini G, De Laurentiis M, Vignati S, Chine S, Lucchi M, Silvestri V. Evaluation of epidermal growth factor-related growth factors and receptors and of neoangiogenesis in completely resected stage I-IIIA non-small-cell lung cancer: amphiregulin and microvessel count are independent prognostic indicators of survival. *Clin Cancer Res*. 1998;4:241-249.
37. Addison CL, Ding K, Zhao H, et al. Plasma transforming growth factor alpha and amphiregulin protein levels in NCIC clinical trials group BR.21. *J Clin Oncol*. 2010;28:5247-5256.
38. Ohchi T, Akagi Y, Kinugasa T, et al. Amphiregulin is a prognostic factor in colorectal cancer. *Anticancer Res*. 2012;32:2315-2321.
39. Jing C, Jin YH, You Z, Qiong Q, Jun Z. Prognostic value of amphiregulin and epiregulin mRNA expression in metastatic colorectal cancer patients. *Oncotarget*. 2016;7:55890-55899.
40. Brown CL, Meise KS, Plowman GD, Coffey RJ, Dempsey PJ. Cell surface ectodomain cleavage of human amphiregulin precursor is sensitive to a metalloprotease inhibitor. Release of a predominant N-glycosylated 43-kDa soluble form. *J Biol Chem*. 1998;273:17258-17268.
41. Bostwick DG, Qian J, Maihle NJ. Amphiregulin expression in prostatic intraepithelial neoplasia and adenocarcinoma: a study of 93 cases. *Prostate*. 2004;58:164-168.
42. Yoshida M, Shimura T, Fukuda S, et al. Nuclear translocation of pro-amphiregulin induces chemoresistance in gastric cancer. *Cancer Sci*. 2012;103:708-715.
43. Mallakin A, Sugiyama T, Kai F, et al. The Arf-inducing transcription factor Dmp1 encodes a transcriptional activator of amphiregulin, thrombospondin-1, JunB and Egr1. *Int J Cancer*. 2010;126:1403-1416.
44. Isokane M, Hieda M, Hirakawa S, et al. Plasma-membrane-anchored growth factor pro-amphiregulin binds A-type Lamin and regulates global transcription. *J Cell Sci*. 2008;121:3608-3618.
45. Busser B, Sancey L, Brambilla E, Coll JL, Hurbin A. The multiple roles of amphiregulin in human cancer. *Biochim Biophys Acta*. 2011;1816(2):119-131.
46. Steponaitis G, Kazlauskas A, Skiriute D, Vaitkiene P, Skauminas K, Tamasauskas A. Significance of amphiregulin (AREG) for the outcome of low and high grade astrocytoma patients. *J Cancer*. 2019;10:1479-1488.
47. Chinot OL, Wick W, Mason W, et al. Bevacizumab plus radiotherapy-temozolomide for newly diagnosed glioblastoma. *N Engl J Med*. 2014;370:709-722.
48. Blasco MA. Telomerase beyond telomeres. *Nat Rev Cancer*. 2002;2:627-633.
49. So WK, Fan Q, Lau MT, Qiu X, Cheng JC, Leung PCK. Amphiregulin induces human ovarian cancer cell invasion by down-regulating E-cadherin expression. *FEBS Lett*. 2014;588:3998-4007.
50. Adam RM, Chamberlin SG, Davies DE. Induction of anchorage-independent growth by amphiregulin. *Growth Factors Chur Switz*. 2016;13:193-120.
51. Menashi S, Serova M, Ma L, Vignot S, Mourah S, Calvo F. Regulation of extracellular matrix metalloproteinase inducer and matrix metalloproteinase expression by amphiregulin in transformed human breast epithelial cells. *Cancer Res*. 2003;63:7575-7580.

## SUPPORTING INFORMATION

Additional supporting information may be found in the online version of the article at the publisher's website.

**How to cite this article:** Maille E, Levallet J, Dubois F, et al. A defect of amphiregulin release predicted longer survival independently of YAP expression in patients with pleural mesothelioma in the IFCT-0701 MAPS phase 3 trial. *Int. J. Cancer*. 2022;1-16. doi:10.1002/ijc.33997